Theoretical study of the He–HF+ complex. I. The two asymptotically degenerate ground state potential energy surfaces

Victor F. Lotrich, Paul E. S. Wormer, and Ad van der Avoird

Citation: J. Chem. Phys. **120**, 93 (2004); doi: 10.1063/1.1629671
View online: http://dx.doi.org/10.1063/1.1629671
View Table of Contents: http://jcp.aip.org/resource/1/JCPSA6/v120/i1
Published by the American Institute of Physics.

Theoretical study of the He–HF^+ complex. I. The two asymptotically degenerate ground state potential energy surfaces

Victor F. Lotrich, Paul E. S. Wormer, and Ad van der Avoird[a)]
Institute of Theoretical Chemistry, NSRIM, University of Nijmegen, Toernooiveld, 6525 ED Nijmegen, The Netherlands

(Received 26 August 2003; accepted 6 October 2003)

Two three-dimensional potential energy surfaces (PESs) are reported for the cationic complex He–HF^+; they are degenerate for linear geometries of the complex and correlate with the doubly degenerate $X\,^2\Pi$ ground state of the HF^+ monomer. The PESs are computed from the interaction energies of the neutral dimer and the ionization potentials of the He–HF complex and the HF molecule. Ionization potentials are obtained from the outer valence Green's function (OVGF) method, while the energies of the neutral species are computed by means of the single and double coupled-cluster method with perturbative triples [CCSD(T)]. For comparison, interaction energies of the ionic complex were computed also by the use of the partially spin-restricted variant of the CCSD(T) method. After asymptotic scaling of the OVGF results, good agreement is found between the two methods. A single global minimum is found in the PES, for the linear He–HF^+ geometry. The well depth and equilibrium separation are 2.240 Å and 1631.3 cm^{-1}, respectively, at an HF^+ bond length $r=1.0012$ Å, in rather good agreement with results of Schmelz and Rosmus [Chem. Phys. Lett. **220**, 117 (1994)]. The well depth depends much more strongly on the internuclear H–F separation than in the neutral He–HF complex and the global minimum in a full three-dimensional PES occurs at $r=1.0273$ Å. © *2004 American Institute of Physics.* [DOI: 10.1063/1.1629671]

I. INTRODUCTION

Over the last decade or so, great progress has been made in the computation of interaction energies between closed-shell systems. We mention two of the approaches that have been particularly successful: the symmetry-adapted perturbation theory (SAPT) developed by Jeziorski *et al.*[1] and the single and double coupled-cluster method with perturbative triples [CCSD(T)],[2] which is a supermolecule method. Recently attention has shifted to dimers that dissociate into a degenerate open-shell monomer and a nondegenerate closed-shell monomer. The asymptotic degeneracy disqualifies both methods: the SAPT as well as the CCSD(T) approach compute correlation corrections to the energy of a single-reference nondegenerate Hartree–Fock ground state, a spin singlet.

A major difficulty in open-shell systems is the adaptation of the wave function to the total spin operator S^2. At present no SAPT method has been formulated that solves this problem, but for the CCSD method a partial circumvention was published by Knowles *et al.*,[3,4] who refer to their method as "partially spin restricted." When moreover triple corrections[5] are included, the spin restricted CCSD(T) method, RCCSD(T), is obtained.

Recently, an alternative method was proposed[6–9] that avoids the consideration of open-shell systems altogether. This method is applicable to dimers that dissociate into a neutral closed-shell system A and an (open-shell) cation B^+. This is the case when the ionization potentials of A and B satisfy $I_A \gg I_B$. The interaction energy $E_{\rm int}^+$ of the ionic complex can then be computed from the interaction energy $E_{\rm int}^0$ of the neutral complex and the ionization potential of the neutral complex (I_{AB}) and of the neutral monomer B (I_B). That is, $E_{\rm int}^+ = E_{\rm int}^0 + \Delta_{\rm int}$, with $\Delta_{\rm int} = I_{AB} - I_B$. Obviously, the ionization potential I_{AB} depends on the geometry of the dimer. We will refer to this method as the ionization potential (IP) method. Although the interaction in the neutral species can be computed by any method, we will use the SAPT and the CCSD(T) method for the reasons mentioned above. The ionization potentials are obtained from the outer valence Green's function (OVGF) method.[10] The IP method was applied in studies of Penning ionization electron spectroscopy.[6–8] It was tested on the Rg–CO^+, Rg=He, Ne, Ar, complexes[9] and it was concluded that after asymptotic scaling it compares extremely well with RCCSD(T) for He–CO^+. Agreement between the two methods for Ne–CO^+, while not as good, indicated that reliable potentials could be obtained using either method. The method did not work as well for Ar–CO^+, because $I_{\rm Ar} \gtrsim I_{\rm CO}$, the values being 15.8 and 14.0 eV, respectively.

The He–HF^+ dimer represents an ideal system to be investigated by the use of the IP method. The ionization potential of He (24.5874 eV)[11] is sufficiently larger than of HF (16.06 eV).[12] The neutral species has been extensively studied and the lowest two, nearly degenerate, potential energy surfaces of He–HF^+ have been previously computed by the coupled electron pair (CEPA) approach and rovibronic levels were obtained. Although the CEPA potentials are expected to

a)Author to whom correspondence should be addressed. Electronic mail: avda@theochem.kun.nl

TABLE I. Convergence of $E_{\rm int}^0$ with basis set. All energies are in $\rm cm^{-1}$ and were computed at $R=2.5$ Å and $r=0.9170$ Å with the SCF and CCSD(T) method.

θ (degrees)	0°		90°		180°	
Basis	SCF	CCSD(T)	SCF	CCSD(T)	SCF	CCSD(T)
aug-cc-pVDZ	564.25	446.28	254.58	209.56	186.92	108.55
aug-cc-pVTZ	526.34	333.62	251.77	164.23	185.89	74.82
aug-cc-pVQZ	524.66	312.23	252.57	151.80	186.22	64.76
aug-cc-pVDZ3321	521.64	325.84	254.21	157.07	187.04	65.55
aug-cc-pVTZ3321	525.42	319.41	252.64	147.75	186.38	60.69
aug-cc-pVQZ3321	524.97	310.36	252.31	144.17	186.10	58.72

be slightly underbound, the general features of the surface should be reliable. In the present paper we wish to extend the IP method, introduced in Ref. 9, by obtaining the two potential energy surfaces that asymptotically coincide with the $X\,^2\Pi$ energies of HF^+. This will allow us to test the IP method against previous computations and RCCSD(T) results.

The interaction of He with HF^+ in the $X\,^2\Pi$ state gives rise to two (adiabatic) potential surfaces of reflection symmetry A' and A''. Two diabatic potentials will be constructed from these and fitted analytically; the appropriate form of the angular expansion functions was given in Refs. 13–15.

The outline of the paper is as follows: In Sec. II computational details are given. It describes the basis sets used and the fits of the diabatic potentials. In Sec. III results for the neutral and ionic dimer are presented and discussed. In particular it is explained how the potential of the ionic dimer may be scaled to obtain correct asymptotic behavior. The paper is ended by Sec. IV containing the conclusions.

II. COMPUTATIONAL DETAILS

The intermolecular potential energy surface of the $He–HF^+$ dimer can be described by three parameters R, θ, and r. The vector **R** points from the helium atom to the center of mass of HF and θ is the angle between **R** and the vector **r** pointing from the hydrogen atom to the fluorine atom. The quantity r is the internuclear HF distance. The center of mass of HF is defined by the masses 1.007825 and 18.9984 u of the hydrogen and fluorine atoms, respectively.

The CCSD(T) and RCCSD(T) calculations in this work have been performed by the use of the MOLPRO package.[16] For comparison sake a number of interaction energies of the linear neutral dimer have also been computed by the SAPT96 package.[17] IPs have been computed by the OVGF method implemented in the GAUSSIAN 98 program.[18] This program returns IPs for requested occupied orbitals. The difference $\Delta'_{\rm int}$, leading to the A' potential energy surface, is $I^{A'}_{\rm He-HF}-I_{\rm HF}$, where $I_{\rm HF}$ is the IP of the highest occupied molecular orbital of HF and $I^{A'}_{\rm He-HF}$ is the IP of the HOMO of He–HF that is of A' symmetry. Likewise, $\Delta''_{\rm int}$, leading to the A'' surface, is obtained by subtracting $I_{\rm HF}$ from the IP of the dimer HOMO of A'' symmetry. In all cases method B[10] of GAUSSIAN 98 was used for the computation of IPs.

A. Basis sets

Basis set requirements may differ for the energies of the neutral complex, the RCCSD(T) energies of the ionic complex, and the ionization potentials of the neutral species. Since we are mostly interested in the ionic interaction energy, we inspected basis set dependences at 2.5 Å, which is close to the ionic equilibrium separation. We stress that all energies—of monomer and dimer—are calculated in the dimer basis, so that automatically the basis set superposition error[19] is corrected for. This procedure is in fact equivalent to the counterpoise correction of Boys and Bernardi.[20]

Inclusion of bond functions is known to significantly increase the rate of convergence of the intermolecular interaction energy with respect to basis size, particularly for dispersion interactions in neutral systems.[21,22] We have therefore studied the effect of bond functions on the convergence of the interaction energies. Placement of the bond functions is not critical[21,22] and we have used the $3s3p2d1f$ set of bond functions of Tao and Pan[23,24] placed at the midpoint of **R**.

The interaction energy $E_{\rm int}^0$ of neutral He–HF has been computed in the aug-cc-pVXZ, X=D,T,Q bases[25] with and without the $3s3p2d1f$ set of midbond functions and results are given in Table I. The correlation contribution to the interaction energy is, as expected, much more sensitive to the basis than the self-consistent field (SCF) energy. Energies computed in the aug-cc-pVDZ basis are clearly not converged. However addition of the bond functions to the aug-cc-pVDZ basis, yielding the aug-cc-pVDZ3321 basis, significantly lowers the interaction energy to within about 10% of the values computed in the largest basis. Addition of bond functions to the aug-cc-pVQZ basis has still some effect. Since the differences between the aug-cc-pVTZ3321 and aug-cc-pVQZ3321 are less than 5%, we conclude that the former basis is adequate for the computation of the potential energy surface of the neutral complex.

The interaction energies in the ionic dimer have been computed in the same basis sets as the interaction energy of the neutral complex, see Table II for results. Bond functions are known[22] to adversely affect electrostatic interaction energies, which are very important in the ionic dimer. We see this confirmed by comparing RCCSD(T) results at $\theta=90°$ in the aug-cc-pVDZ and aug-cc-pVDZ3321 basis, -326.48 and $-222.74\ \rm cm^{-1}$, respectively. Since the corresponding number in the aug-cc-pVQZ basis is $-343.13\ \rm cm^{-1}$, we find that addition of bond functions deteriorates the result. The

TABLE II. Convergence of $E_{\rm int}^+$ (A' symmetry) with basis set. All energies are in cm^{-1} and were computed at $R=2.5$ Å and $r=0.9170$ Å with the SCF and RCCSD(T) method.

θ (degrees)	0°		90°		180°	
Basis	SCF	RCCSD(T)	SCF	RCCSD(T)	SCF	RCCSD(T)
aug-cc-pVDZ	−703.27	−844.66	−227.10	−326.48	−8.01	−81.50
aug-cc-pVTZ	−781.91	−977.70	−209.19	−326.31	−2.16	−100.67
aug-cc-pVQZ	−785.16	−995.48	−219.01	−343.13	−3.30	−108.83
aug-cc-pVDZ3321	−796.11	−1005.75	−158.90	−222.74	−6.43	−118.32
aug-cc-pVTZ3321	−785.24	−991.30	−195.00	−280.60	−4.87	−113.79
aug-cc-pVQZ3321	−784.98	−996.56	−216.15	−329.69	−4.67	−114.30

SCF interaction energy shows similar behavior. Because of this adverse effect, we have computed the RCCSD(T) energies of He–HF$^+$ in the aug-cc-pVQZ basis.

The ionization potentials have been computed in the aug-cc-pVXZ (X=D,T,Q) bases. Bond functions have not been included, for here, too, unphysical results were obtained upon addition of such functions. Table III shows the $\Delta'_{\rm int}$ values obtained from the OVGF method. Convergence of the ionization potential $I_{\rm HF}$ of HF is also shown; it is not very sensitive to the basis, varying only 0.06 eV in the bases considered. The experimental values are 16.06 and 16.19 eV[12] for the adiabatic and vertical ionization energies, respectively. The latter is 3% lower than our aug-cc-pVQZ value. The difference is partly due to the value of r used, $1.7328\,a_0$ ($=0.9170$ Å). If we compute the ionization potential at the average r value for the ground state of HF ($r_0=1.77176\,a_0$) it is lower by 0.07 eV. Table III indicates that $\Delta'_{\rm int}$ should be computed in at least the aug-cc-pVTZ basis. Since results in this basis differ only 1.1%, 0.3%, and 3.3% from those obtained in the aug-cc-pVQZ basis we have computed the full $\Delta'_{\rm int}$ and $\Delta''_{\rm int}$ surfaces in the aug-cc-pVTZ basis.

In Ref. 26 a SAPT potential energy surface was reported for neutral He–HF. A multipole expanded dispersion energy was computed in the basis $5s4p3d2f$ for He and $6s5p4d3f2g/5s4p3d2f$ for HF and used to scale the SAPT interaction energy that was computed in a smaller basis. In this work we used the larger basis for all SAPT calculations of the neutral complex. This larger basis is comparable to the aug-cc-pVTZ basis.

B. Potential energy fits

We write $V_{A'}$ for $E_{\rm int}^+$ when the ionization is from an A' orbital, and the dimer has A' symmetry accordingly. An equivalent definition holds for $V_{A''}$. As described above we computed the $V_{A'}$ and $V_{A''}$ surfaces. The nuclear kinetic energy becomes singular for linear geometries. This problem can be avoided by transformation of the A' and A'' adiabatic states to a set of diabatic states.[15] The required transformation is the one that transforms the Π_x and Π_y states of the hydrogen fluoride cation to eigenstates Π_1 and Π_{-1} of the electronic angular momentum operator L_z. This leads to the following unitary transformation of the potential

$$\frac{1}{2}\begin{pmatrix}-1 & i\\ 1 & i\end{pmatrix}\begin{pmatrix}V_{A'} & 0\\ 0 & V_{A''}\end{pmatrix}\begin{pmatrix}-1 & 1\\ -i & -i\end{pmatrix}$$

$$=\frac{1}{2}\begin{pmatrix}V_{A'}+V_{A''} & V_{A''}-V_{A'}\\ V_{A''}-V_{A'} & V_{A'}+V_{A''}\end{pmatrix}\equiv\begin{pmatrix}V_{1,1} & V_{1,-1}\\ V_{-1,1} & V_{-1,-1}\end{pmatrix}.$$

The 2×2 matrix on the right hand side is referred to as the diabatic potential. So, instead of fitting $V_{A'}$ and $V_{A''}$, we fit the plus and minus combinations. By means of symmetry arguments it is shown in Ref. 15 that $V_{1,1}$ ($=V_{-1,-1}$) must be fitted in terms of ordinary Legendre polynomials $P_l^0(\theta)=P_l(\cos\theta)$ and $V_{-1,1}$ ($=V_{1,-1}$) in terms of associated Legendre functions $P_l^2(\theta)$. We decompose the potential into a short and a long range part

$$V_{\pm1,1}=V_{\pm1,1}^{\rm SR}+V_{\pm1,1}^{\rm LR}, \tag{1}$$

which we fit separately. We fit $V_{\pm1,1}^{\rm LR}$ to the total interaction energy for $R\geqslant6$ Å and define $V_{\pm1,1}^{\rm SR}$ as the difference between the total interaction energy and the long range energy extrapolated to values $R<6$ Å.

TABLE III. Convergence of $\Delta'_{\rm int}\equiv I^{A'}_{\rm He-HF}-I_{\rm HF}$ with basis set, where $I^{A'}_{\rm He-HF}$ is the first IP for ionizing from an orbital of A' symmetry. All energies are in cm^{-1} and were computed at $R=2.5$ Å and $r=0.9170$ Å with the OVGF method. The ionization potential $I_{\rm HF}$ of HF is in eV.

Basis	$\theta=0°$	$\theta=90°$	$\theta=180°$	$I_{\rm HF}$
aug-cc-pVDZ	−1247.32	−361.74	−135.10	16.794
aug-cc-pVTZ	−1245.47	−456.40	−115.10	16.745
aug-cc-pVQZ	−1232.32	−442.63	−111.38	16.730

1. Long range

As stated, the long range coefficients have been obtained by fitting $V_{\pm1,1}^{\rm LR}$ for $R\geqslant6$ Å. We used the forms

$$V_{1,1}^{\rm LR}=\sum_{n=4}^{9}\sum_{l=0}^{l_{\max}}\sum_{k=0}^{2}P_l^0(\theta)R^{-n}D_n(\beta_nR)r^ks_{nlk}, \tag{2}$$

and

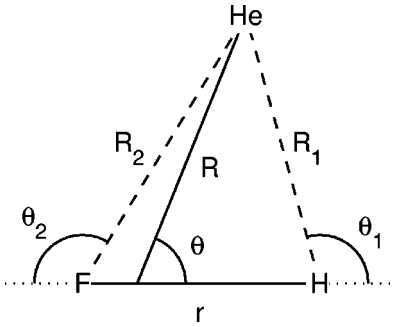

FIG. 1. Variables used in the SR potential energy fits, cf. Eqs. (5) and (6). Note that $R \equiv R_0$ and $\theta \equiv \theta_0$.

$$V_{-1,1}^{\mathrm{LR}} = \sum_{n=6}^{9} \sum_{l=2}^{l_{\max}} \sum_{k=0}^{2} P_l^2(\theta) R^{-n} D_n(\beta_n R) r^k d_{nlk}. \tag{3}$$

Here $D_n(\beta_n R)$ are Tang–Toennies damping functions

$$D_n(z) = 1 - \exp(-z) \sum_{k=0}^{n} \frac{z^k}{k!}, \tag{4}$$

which were set equal to one while obtaining the coefficients s_{nlk} and d_{nlk}. The nonlinear damping parameters β_n for $n = 4,\ldots,9$ were determined in the global fit of all points. However, the values of β_8 and β_9 were not independently varied, they were set equal to β_6 and β_7, respectively. In Eqs. (2) and (3) s_{nlk} and d_{nlk} are nonzero only for $l \leqslant n-4$ and l must be even (odd) for even (odd) values of n.

The contribution $C_4 R^{-4}$ is proportional to the charge on the HF^+ and the polarizability of the helium atom, neither of which are functions of r. Therefore in Eq. (2) the sum is restricted to $k=0$ when $n=4$. It is relevant for the subsequent discussions to point out that the contributions for $n \leqslant 5$ contain only induction while those for $n>5$ contain induction as well as dispersion contributions.

2. Short range

Expansions of the off-diagonal elements of the diabatic potential in $P_l^2(\theta)$ required expansions with very high values of $l_{\max}$ which invariably contained oscillations. In order to remedy this we have used the variables (R_1, θ_1), and (R_2, θ_2) as well as (R, θ) in separate expansions, where R_1, R_2, θ_1, and θ_2 are defined in Fig. 1. Using these variables we were able to obtain accurate fits which were free from oscillations. In order to obtain a compact representation of the functional form, we introduce $R_0 \equiv R$ and $\theta_0 \equiv \theta$, and write

$$V_{1,1}^{\mathrm{SR}} = \sum_{k=0}^{2} r^k \exp(-hr) \sum_{l=0}^{1} P_l^0(\theta) \times \sum_{i=0}^{2} \exp[-A_i(\theta_i) R_i] \sum_{n=0}^{2} s_{ilkn} R_i^n, \tag{5}$$

with

$$A_i(\theta_i) = a_{0i} + a_{1i} \cos\theta_i.$$

The form for $V_{-1,1}^{\mathrm{SR}}$ is

$$V_{-1,1}^{\mathrm{SR}} = \sum_{k=0}^{2} r^k \exp(-hr) \sum_{l=2}^{3} P_l^2(\theta) \times \sum_{i=0}^{2} \exp[-B_i(\theta_i) R_i] \sum_{n=0}^{2} d_{ilkn} R_i^n, \tag{6}$$

with

$$B_i(\theta_i) = b_{0i} + b_{1i} \cos\theta_i.$$

Note that h is a fitting parameter common to both expansions, whereas s_{ilkn} and a_{ji} are determined from a fit of $V_{1,1}^{\mathrm{SR}} \equiv (V_{A'}^{\mathrm{SR}} + V_{A''}^{\mathrm{SR}})/2$. Similarly, d_{ilkn} and b_{ji} are determined from a fit of $V_{-1,1}^{\mathrm{SR}} \equiv (V_{A''}^{\mathrm{SR}} - V_{A'}^{\mathrm{SR}})/2$.

To inspect the quality of the fit we compared fitted values F_i to original values O_i of $V_{1,1}$ and $V_{-1,1}$ for $R = 1.5$, 2.5, 6.0 Å, which are in the repulsive, bonding, and LR region, respectively. As a measure we take

$$\mathrm{rms} = \left[\frac{1}{N} \sum_{i=1}^{N} \left(\frac{O_i - F_i}{O_i} \right)^2 \right]^{1/2} \quad \text{with} \quad O_i \neq 0.$$

In the case of $V_{1,1}$ we have $N=39$ (3 values of r and 13 θ values), while for $V_{-1,1}$ we have 33 nonvanishing points. The $V_{1,1}$ rms values are 0.29%, 0.17%, and 0.12% for

TABLE IV. Contributions to the interaction of the linear He–HF ($\theta = 0°$) for intermolecular separations R around the minimum; $r = 0.9170$ Å. Energies in mhartree.

R (a_0)	5.0	5.5	6.0	6.5	8.0	10.0
$E_{\mathrm{disp}}^{(2)}(2)$[a]	−1.1065	−0.5677	−0.3017	−0.1671	−0.0370	0.0080
$E_{\mathrm{disp}}^{(2)}$(ASDE)[b]	−1.0749	−0.5422	−0.2839	−0.1552	−0.0336	−0.0075
E_{int}^{0}[SAPT-L][a]	0.5620	−0.0815	−0.1858	−0.1588	−0.0495	−0.0111
E_{int}^{0}[CCSD(T)]	0.4811	−0.1146	−0.1993	−0.1625	−0.0487	−0.0107
E_{int}^{0}[SAPT-M][b]	0.6006	−0.0615	−0.1738	−0.1490	−0.0470	−0.0108
E_{int}^{0}[LN][c]	0.5824	−0.0661	−0.1716	−0.1503	−0.0498	−0.0119
E_{int}^{0}[LN*]	0.4977	−0.1144	−0.1985	−0.1652	−0.0524	−0.0122

[a]Computed in present work.
[b]Asymptotically scaled energy from Ref. 26.
[c]From the HFD2 potential of Rodwell *et al.* as modified by Lovejoy and Nesbitt.

TABLE V. Contributions to the interaction of the linear He–FH ($\theta=180°$) for intermolecular separations R around the minimum; $r=0.9170$ Å. Energies in mhartree.

R (a_0)	5.0	5.5	6.0	6.5	8.0	10.0
$E^{(2)}_{\rm disp}(2)$[a]	−0.5245	−0.2806	−0.1572	−0.0922	−0.0236	−0.0058
$E^{(2)}_{\rm disp}$(ASDE)[b]	−0.6339	−0.3241	−0.1755	−0.1088	−0.0256	−0.0061
$E^0_{\rm int}$[SAPT-L][a]	0.0198	−0.1173	−0.1110	−0.0812	−0.0253	−0.0065
$E^0_{\rm int}$[CCSD(T)]	0.0156	−0.1135	−0.1079	−0.0793	−0.0244	−0.0062
$E^0_{\rm int}$[SAPT-M][b]	−0.0913	−0.1606	−0.1297	−0.0905	−0.0278	−0.0069
$E^0_{\rm int}$[LN][c]	−0.0456	−0.1528	−0.1318	−0.0931	−0.0287	−0.0071
$E^0_{\rm int}$[LN*]	0.0391	−0.1045	−0.1048	−0.0782	−0.0260	−0.0067

[a]Computed in present work.
[b]Asymptotically scaled energy from Ref. 26.
[c]From the HFD2 potential of Rodwell *et al.* as modified by Lovejoy and Nesbitt.

$R=1.5$, 2.5, 6.0 Å, respectively, and those of the much smaller difference potential $V_{-1,1}$ are 3.1%, 5.1%, and 4.7%.

III. RESULTS AND DISCUSSION

The neutral interaction energy $E^0_{\rm int}$ and the values of $\Delta'_{\rm int}$ and $\Delta''_{\rm int}$ have been computed at $R=1.5$, 2.0, 2.5, 3.0, 3.5, 4, 5, 6, 8, and 10 Å. At each value of R the angle θ was varied from 0° to 180° with steps of 15°. This (R,θ) scan was performed for $r=0.9170$, 1.0012, and 1.0823 Å. This leads to a total of 390 points that were all included in the fitting procedure. The raw numbers are available upon request.

The SAPT calculations of the neutral interaction energy $E^0_{\rm int}$ were performed at linear geometries for $R=5$, 5.5, 6, 6.5, 8, and 10 a_0. The bond length r was fixed at 1.7328 a_0; the large basis used earlier for asymptotic scaling[26] was applied. Results of these SAPT-L computations are reported in Tables IV and V in the rows labeled by $E^0_{\rm int}$[SAPT-L].

The RCCSD(T) computations for He–HF^+, which are meant to gauge the IP method, have been restricted to the symmetric A' state and one r value (0.9170 Å). Radial scans were done at $\theta=0°$, 90°, 180° for intermolecular separations 1.5 2, 2.5, 3, 3.5, 4, 5, 6, 8, and 10 Å. Angular scans were performed at $R=2.5$ and 6 Å for $\theta=0°$, 30°, 60°, 90°, 120°, 150°, and 180°. Results of the RCCSD(T) and IP method are compared in Tables VI, VII, and VIII for $\theta=0°$, 90°, and 180°, respectively, and in Figs. 4 and 5 for $R=2.5$ and 6 Å.

A. Intermolecular potential of the neutral dimer

Accurate computation of the interaction energy of the neutral dimer is critical if we are to obtain reliable potential energy surfaces for the cationic dimer by the IP method. The neutral He–HF system has been the subject of extensive *ab initio* and experimental studies and several potential energy surfaces exist. The most accurate of these are the potential of Moszynski *et al.*,[26] computed by symmetry adapted perturbation theory (SAPT-M), and the semiempirical surface of Lovejoy and Nesbitt (LN).[27] These potentials agree well with each other and reproduce observed near-infrared transitions. Comparison of our computations to the SAPT-M potential reveals some unexpected disagreement which we will now address.

In Tables IV and V we compare intermolecular interaction energies computed at the CCSD(T) level to SAPT-M[26] and LN[27] results. We also list the present (SAPT-L) results. At $\theta=0°$ all interactions agree reasonably well. However, at $\theta=180°$ the results differ significantly for the smaller R values. In fact CCSD(T) predicts a secondary minimum (at $\theta=180°$) about 50% shallower than the primary minimum ($\theta=0$), whereas the SAPT-M potential predicts these two minima to be about equally deep. The LN potential shows the same behavior as the SAPT-M potential, (see also Fig. 2).

Disagreement between the CCSD(T) energies and $E^0_{\rm int}$[LN] can easily be explained by analyzing the model that Lovejoy and Nesbitt used to construct the potential. They started from the Hartree–Fock plus damped dispersion po-

TABLE VI. Interaction energies at $\theta=0$ of neutral He–HF and of the ground A' state of He–HF^+ from the IP, the scaled IP, and the RCCSD(T) method. Energies are in cm^{-1} and $r=0.9170$ Å.

R (Å)	$E^0_{\rm int}$	$V_{A'}$	$V^{\rm sc}_{A'}$	$E^+_{\rm int}$[RCCSD(T)]
1.5	38 524.75	28 000.70	27 247.47	27 187.31
2.0	4 042.98	−119.47	−349.78	−290.89
2.5	310.36	−935.11	−1041.02	−995.48
3.0	−37.63	−420.23	−471.67	−460.52
3.5	−33.06	−177.82	−206.37	−203.40
4.0	−15.68	−85.08	−101.27	−100.30
5.0	−3.50	−27.10	−33.66	−33.27
6.0	−1.04	−11.26	−14.49	−14.20
8.0	−0.17	−3.05	−4.02	−3.92
10.0	−0.04	−1.15	−1.53	−1.49

TABLE VII. Interaction energies at $\theta=90°$ of neutral He–HF and of the ground A' state of He–HF^+ from the IP, the scaled IP, and the RCCSD(T) method. Energies are in cm^{-1} and $r=0.9170$ Å.

R (Å)	$E^0_{\rm int}$	$V_{A'}$	$V^{\rm sc}_{A'}$	$E^+_{\rm int}$[RCCSD(T)]
1.5	13 451.06	2068.22	1880.23	2201.14
2.0	1 654.93	−442.99	−579.60	−470.21
2.5	144.16	−312.23	−389.57	−343.13
3.0	−11.87	−147.64	−188.57	−172.44
3.5	−14.35	−72.53	−94.57	−90.46
4.0	−7.60	−38.60	−51.91	−50.80
5.0	−1.97	−14.56	−20.07	−19.16
6.0	−0.63	−6.83	−9.50	−9.18
8.0	−0.11	−2.13	−2.96	−2.90
10.0	−0.03	−0.87	−1.20	−1.19

TABLE VIII. Interaction energies at $\theta=180°$ of neutral He–HF and of the ground A' state of $He–HF^+$ from the IP, the scaled IP, and the RCCSD(T) method. Energies are in cm^{-1} and $r=0.9170$ Å.

R (Å)	E^0_{int}	$V_{A'}$	$V^{sc}_{A'}$	E^+_{int}[RCCSD(T)]
1.5	12 606.65	13 296.60	12 912.45	13 087.24
2.0	1 281.82	1 074.32	994.31	991.06
2.5	58.71	−56.40	−107.70	−108.83
3.0	−25.94	−78.77	−106.49	−110.93
3.5	−15.96	−44.87	−60.51	−64.22
4.0	−7.65	−25.68	−35.34	−37.61
5.0	−1.98	−10.31	−14.57	−15.34
6.0	−0.65	−4.98	−7.13	−7.47
8.0	−0.11	−1.64	−2.35	−2.43
10.0	−0.03	−0.70	−1.00	−1.02

tential of Rodwell *et al.*,[28] in which the multipole expanded dispersion is damped in order to account for charge penetration effects. The multipole expansion of Ref. 27 contains C_n dispersion coefficients for $n=6,8,10,12,14$, but the only odd term in the expansion is the $n=7$ term. When we introduce the complete $n=9$ and $n=11$ terms into the expansion of the dispersion energy we obtain the results displayed in Fig. 2 (curve labeled LN*). It is seen that the higher odd terms change the anisotropy of the potential significantly. Tables IV and V show this as well. As appears from these tables and from Fig. 2, the SAPT-M potential disagrees not only with the CCSD(T) computations but also with the improved LN potential E^0_{int}[LN*]. Our SAPT-L results agree quite well with the CCSD(T) and LN* potentials. The older SAPT-M computations were done in a rather small basis. Since dispersion energy converges slowly with basis, Moszynski *et al.*[26] scaled it to have the correct asymptotic behavior.

In Tables IV and V we compare the present dispersion energy $E^{(2)}_{disp}$ with the asymptotically scaled results of Moszynski *et al.*, which are designated by $E^{(2)}_{disp}$ (ASDE). At the linear He–HF geometry the computations agree well. At the linear He–FH geometry, however, these two quantities differ significantly. The difference in the dispersion energy is almost the same as the difference in the total interaction energies. It appears that asymptotic scaling introduces an asymmetry in the potential, which fortuitously coincides with the semiempirical LN potential.

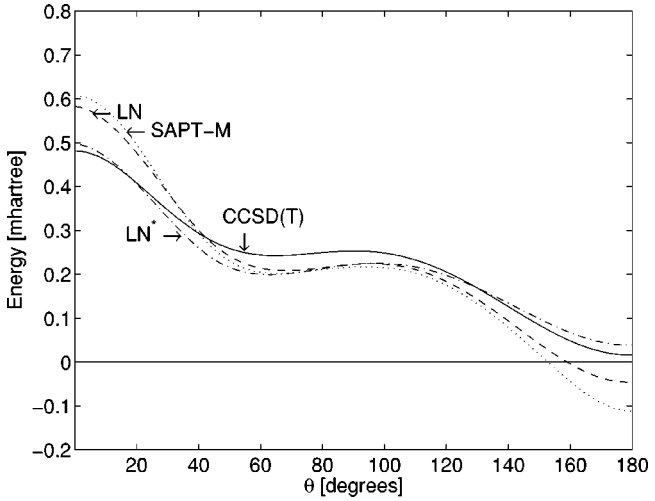

FIG. 2. Interaction energies of neutral He–HF for $R=5\,a_0$ calculated by different methods: SAPT-M is from Moszynski *et al.* (Ref. 26), LN is from Lovejoy and Nesbitt (Ref. 27), LN* is LN with dispersion added in the present work, and CCSD(T) is from present work. Bond distance r of HF is 0.9170 Å.

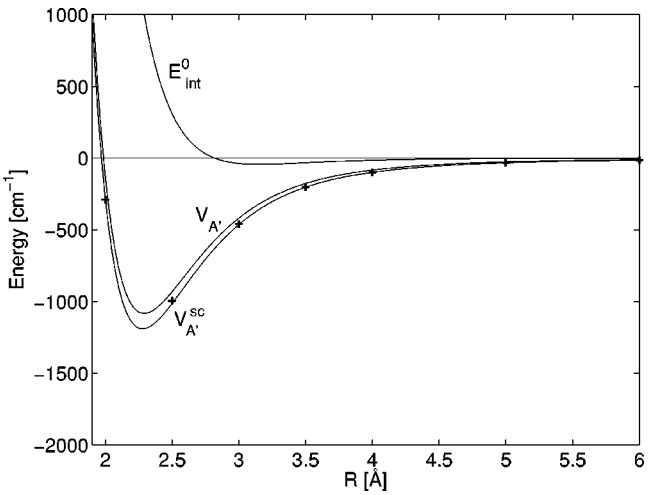

FIG. 3. Interaction energies of neutral He–HF (E^0_{int}) at $\theta=0$ and of $He–HF^+$ with A' symmetry. The energy $V^{sc}_{A'}$ is scaled. RCCSD(T) results are represented by crosses. $r=0.9170$ Å.

B. Intermolecular potential of the cationic dimer

The radial dependence of the neutral E^0_{int} and ionic interaction energies $V_{A'}$ for $\theta=0°$, 90°, and 180° can be seen in Tables VI, VII, and VIII, respectively, and in Fig. 3. Recalling that the absolute minimum in the PES of the neutral system is $-39.7\ cm^{-1}$,[26] this figure shows that the ionic complex is much more strongly bound than the neutral one (by about a factor of 40) and that the R value of the minimum is about 1 Å smaller in the ionic complex than in the neutral. Only for $\theta=180°$ the difference is much less. Since the helium atom is here in close contact with the fluorine atom, this is to be expected. The large binding in the ionic complex is due almost entirely to induction effects, which are accounted for in the IP method.

The A' energies $V_{A'}$ $(\equiv E^0_{int}+\Delta'_{int})$ and E^+_{int}[RCCSD(T)] agree very well in the repulsive region of the potential where exchange effects dominate the interactions, the difference being less than 3% at $R=1.5$ Å. The agreement becomes progressively worse with increasing R until about 4 Å, after which the relative difference remains fairly constant and large. Differences at $R=10$ Å are 30%, 37%, and 46% at $\theta=0°$, 90°, and 180°. These observations indicate that the induction contribution to the interaction energy is substantially underestimated by the IP method, or more precisely, by the OVGF method that is used to compute the geometry-dependent ionization energy of the He–HF complex. In contrast to the $Rg–CO^+$ cations,[9] the anisotropy

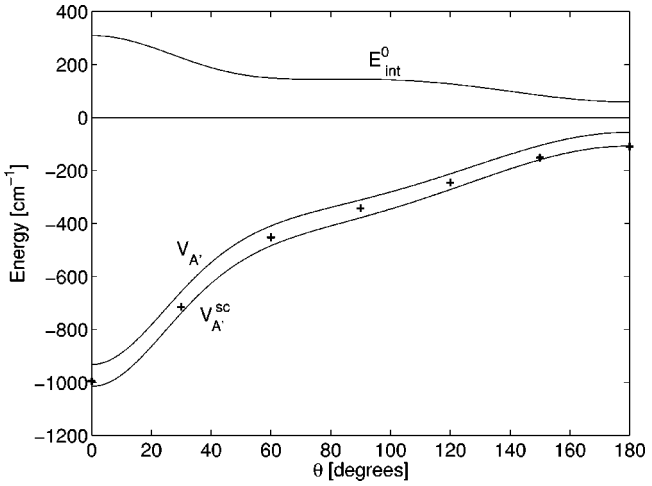

FIG. 4. Intermolecular interaction energies (A' symmetry) at $R=2.5$ Å. Energy E^0_{int} of He–HF and scaled and unscaled energies of He–HF$^+$ computed by the IP method. RCCSD(T) results are represented by crosses. $r=0.9170$ Å.

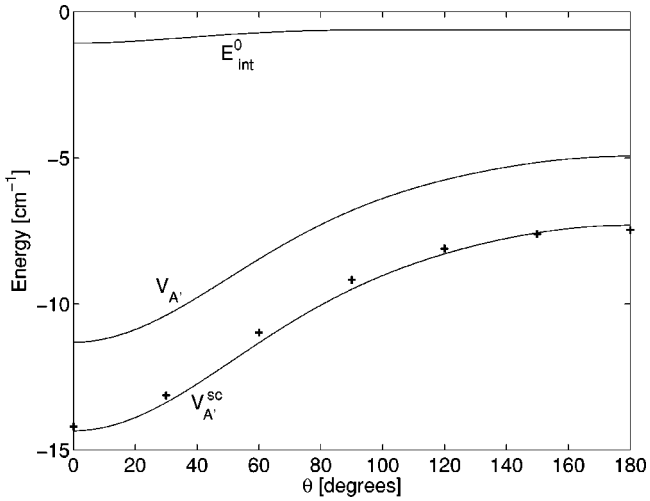

FIG. 5. Intermolecular interaction energies (A' symmetry) at $R=6.0$ Å. Energy E^0_{int} of He–HF and scaled and unscaled energies of He–HF$^+$ computed by the IP method. RCCSD(T) results are represented by crosses. $r=0.9170$ Å.

of the difference suggests that not only the isotropic C_4 contribution is underestimated, but also the anisotropic C_5 contribution. We will return to this below.

C. Scaling of the interaction energy of the cationic dimer

A scaling method that corrects for the underestimate of the induction contribution, particularly at long distances, was introduced in Ref. 9. It was shown that the correct asymptotic behavior is obtained by replacing the long range induction terms in the interaction energy obtained from a fit of the IP method, with the corresponding accurate terms. As we remarked above, only the C_4 and C_5 coefficients contain exclusively induction contributions, which can be expressed as

$$E^+_{\text{ind}}(R,\theta)=C_4R^{-4}+C_5R^{-5}\cos\theta. \tag{7}$$

Here the first term is the charge-induced dipole interaction energy and the second term is the mixed charge/dipole-induced dipole interaction. The coefficients C_4 and C_5 contain the polarizability α of He, the charge $Q=1$ of HF$^+$, and the dipole moment μ of HF$^+$,

$$C_4=-\tfrac{1}{2}\alpha Q^2, \tag{8}$$

$$C_5=2\alpha Q\mu. \tag{9}$$

The isotropic C_4 obtained from the long range fit, cf. Eq. (2), was scaled by the factor

$$\sigma_4=-\tfrac{1}{2}\alpha Q^2/C_4, \tag{10}$$

where the accurate polarizability α used ($1.3831\ a_0^3$) was the explicitly correlated value of Ref. 29. The resulting σ_4 is 1.4163. Scaling the C_5 coefficient was slightly more complicated, as the dipole moment μ of HF$^+$ is a function of r. In order to obtain the scaling factor σ_5 as a function of r we computed $\mu(r)$ at the three values of r used throughout this work. Computations were performed in the aug-cc-pVTZ basis at the multireference configuration interaction level. The scaling factor $\sigma_5(r_i)$ was computed from

$$\sigma_5(r_i)=2\alpha Q\mu(r_i)/C_5(r_i), \tag{11}$$

where again $C_5(r_i)$ is obtained from the LR fit. The three computed values were then fitted to a simple parabolic form

$$\sigma_5(r)=s_0+s_1r+s_2r^2. \tag{12}$$

The shape of the long range anisotropy of the IP is not significantly affected by the scaling of C_4 and C_5, as Fig. 5

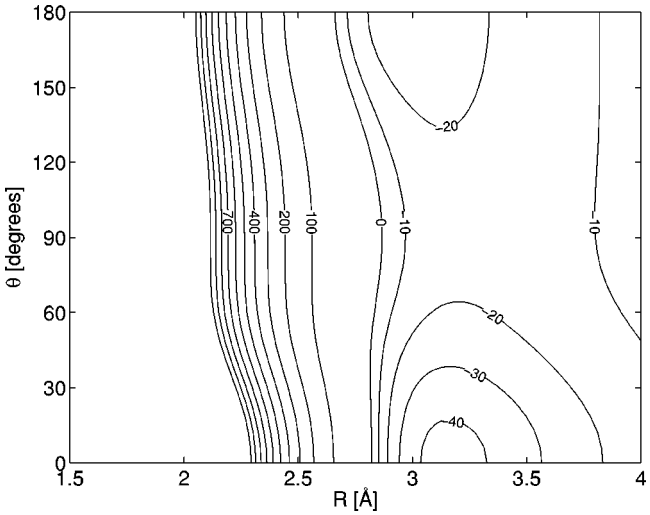

FIG. 6. Potential energy surface E^0_{int} of neutral He–HF computed by the CCSD(T) method. $r=0.9170$ Å. Energy in cm^{-1}.

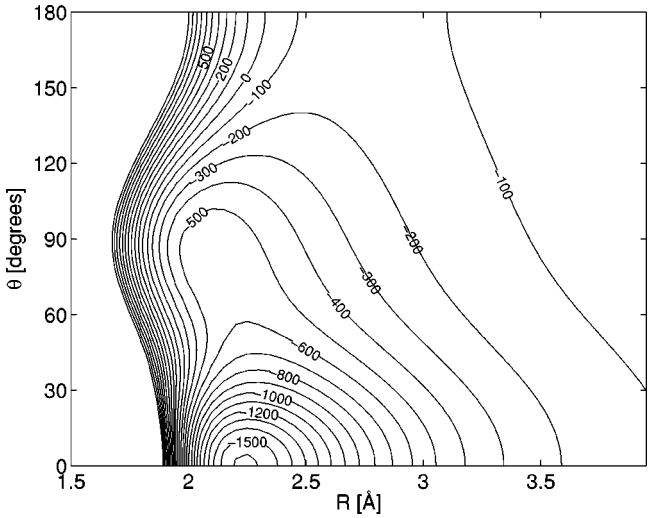

FIG. 7. Adiabatic potential energy surface $V_{A'}^{sc}$ of He–HF^+ computed by the scaled IP method. Symmetry: A', $r=1.0$ Å. Energy in cm^{-1}.

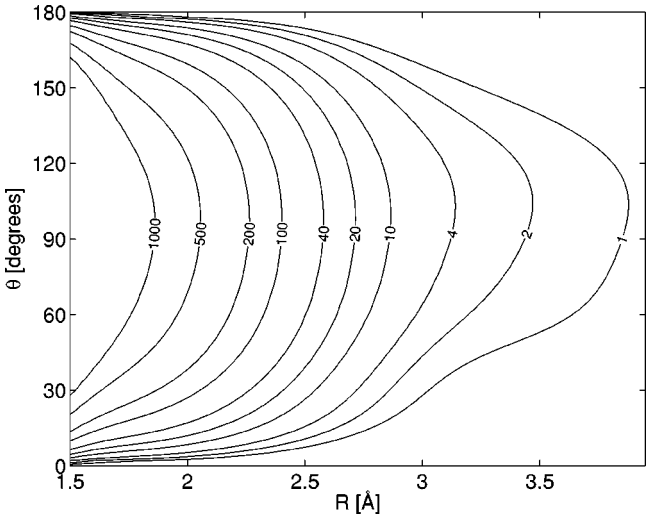

FIG. 9. Diabatic interaction energy $V_{-1,1}^{sc}\equiv(V_{A''}^{sc}-V_{A'}^{sc})/2$ computed by the scaled IP method, in cm^{-1}, for $r=1.0$ Å.

shows, however its magnitude is. The scaled interaction energy, designated by $V_{A'}^{sc}$, is in much better agreement with E_{int}^{+}[RCCSD(T)] at large R. Tables VI–VIII and Figs. 3–5 clearly show this, the maximum difference being 7% for intermolecular separations larger than 5 Å.

Scaling has little effect on the IP method energy in the repulsive region as Tables VI–VIII show. The absolute error is largest at $R=1.5$ Å and $\theta=0°$, but as Fig. 3 shows, the scaled potential nearly coincides with the unscaled one in the highly repulsive region. The differences between the scaled potential and the RCCSD(T) computations are generally less than 10% and at the linear He–HF geometry, where the interaction is strongest, less than 5%. As seen in Fig. 4, the anisotropy is well described.

Overall, the scaling of the potential significantly increases the well depth (by about 10% at $\theta=0$). The anisotropy of the potential is, however, not changed much. We may conclude that the scaling of the IP leads to much better agreement with RCCSD(T) computations of the ionic interaction energy, particularly at large intermolecular separations.

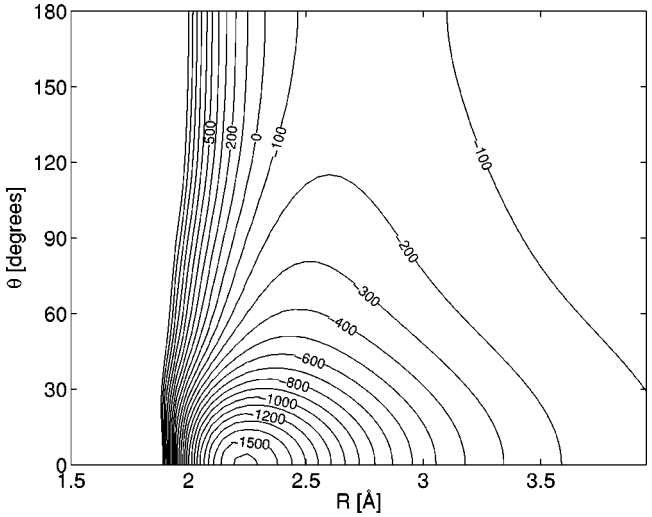

FIG. 8. Adiabatic potential energy surface $V_{A''}^{sc}$ of He–HF^+ computed by the scaled IP method. Symmetry: A'', $r=1.0$ Å. Energy in cm^{-1}.

D. 3D intermolecular potentials of He–HF and He–HF^+

As can be seen in Fig. 6, the neutral He–HF complex has a shallow global minimum at the linear He–HF ($\theta=0°$) geometry, which is only slightly dependent on the HF bond length r. The depth of the global minimum differs by less than 1 cm^{-1} and the equilibrium separation R_e by 0.11 Å for r values of 0.9170 and 1.0823 Å. The secondary minimum for linear He–FH ($\theta=180°$) is affected even less and in general for large angles the PES is very insensitive to r.

By contrast, the potentials of the ionic He–HF^+ complex (see Figs. 7 and 8) possess a very deep single minimum at the linear He–HF^+ ($\theta=0°$) geometry. The depth of this global minimum varies strongly with r. At $r=0.9170$ Å the binding energy is 1236.1 cm^{-1}, at $r=1.0823$ Å it is 2188.5 cm^{-1}. In order to determine the global minimum in the three dimensional (3D) potential it is necessary to add the intramolecular HF^+ interaction to the intermolecular PES. We modeled the former with the Morse potential

$$V_{intra}(r)=D_e(1-\exp[-\beta(r-r_e)])^2$$

with $r_e=1.0012$ Å. By repeatedly solving the one-dimensional vibrational problem in the potential $V_{intra}(r)$ the parameters D_e and β were optimized so that reasonable values of the rotational constants B_v, $v=0,1,2$ and the vibrational constants ω_e and $\omega_e x_e$ were obtained. The values $\beta=2.2790$ $Å^{-1}$ and $D_e=26\,100.0$ cm^{-1} give $B_v=17.19$, 16.41, 15.61 cm^{-1} which may compared with the experimental numbers of Ref. 30: $B_v=17.14$, 16.28, 15.45 cm^{-1}. The calculated values $\omega_e=3090.5$ cm^{-1} and $\omega_e x_e$

$=91.5\ cm^{-1}$ can be compared with 3090.5 and 89.0.[30] The minimum in the total 3D potential is at $R=2.231$ Å and $r=1.0273$ Å and the well depth of the intermolecular potential at this geometry is $1790.3\ cm^{-1}$ (an increase of $159.0\ cm^{-1}$ with respect to the value for $r=r_e$). The intramolecular energy of HF^+ is raised by $87.0\ cm^{-1}$ with respect to its equilibrium value; the dissociation energy of the complex with respect to HF^+ in its equilibrium geometry is $1703.6\ cm^{-1}$.

Figures 7 and 8 show contour plots of the ionic intermolecular potentials obtained. Figure 7 shows the potential surface of A' symmetry at an r value (1.0 Å) close to the minimum, while Fig. 8 shows the potential for the state of A'' symmetry at the same r value. For the linear geometries ($\theta=0°$ and 180°) the two surfaces coincide, of course, and the difference between them is largest near $\theta=90°$. Figure 9 shows a contour plot of the difference potential ($V^{sc}_{-1,1}\equiv(V^{sc}_{A''}-V^{sc}_{A'})/2$). We have not displayed the average potential $V^{sc}_{1,1}\equiv(V^{sc}_{A'}+V^{sc}_{A''})/2$ because it is not qualitatively different from Figs. 7 and 8.

IV. CONCLUSIONS

Adiabatic intermolecular potential energy surfaces of A' and A'' symmetry of the He–HF^+ complex have been computed by the IP method, that is, as the sum of the neutral He–HF interaction energy and the difference in the geometry-dependent ionization potentials of the He–HFcomplex and the HF molecule. Diabatic potentials (average and difference potentials) have been fitted to a functional form that correctly describes the large R asymptotics and the behavior at and near linear geometries. Accuracy of the neutral interaction energy is mandatory if the method is to be reliable. The neutral interaction energy was seen to differ significantly from both the SAPT-M potential of Moszynski *et al.*[26] and the semiempirical potential of Lovejoy and Nesbitt.[27] When the semiempirical potential of Lovejoy and Nesbitt is corrected to include higher-order dispersion coefficients, very nice agreement was obtained with the large basis CCSD(T) interaction energies. Also SAPT-L computations performed in a large basis agreed well with our CCSD(T) computations indicating that our neutral interaction energies are accurate and that the SAPT-M potential of Moszynski *et al.* describes the anisotropy of the neutral interaction less accurately.

Adiabatic ionic interaction energies of A' symmetry were computed using the RCCSD(T) method as well. Interaction energies obtained from the IP method agree well with the results of the RCCSD(T) calculations at small intermolecular distances R but differ considerably at large and intermediate intermolecular separations. This is due to the underestimate of the induction effects by the OVGF method used to compute the ionization energies required by the IP approach. The large R behavior of the difference in ionization energies can be improved by scaling the first few terms in the multipole expansion of the induction energy with accurate values. Interaction energies $V^{sc}_{A'}$, obtained from the scaled IP method are in good agreement with the RCCSD(T) results for the whole range of R values. The scaling does not strongly affect the anisotropy of the potential surface, which was fairly well represented by the unscaled IP method already.

As expected, the ionic complex is much more strongly bound than the neutral one and the equilibrium separation is shifted considerably inwards. By contrast to the neutral species, the ionic potential energy surface only contains a minimum for the linear He–HF^+ geometry, which is very sensitive to the HF^+ bond length. The equilibrium distance R_e and well depth D_e at the experimental H–F separation (1.0012 Å) were found to be 2.240 Å and $1631.3\ cm^{-1}$, which agrees well with the values of 2.249 Å and $1490\ cm^{-1}$ obtained by Schmelz and Rosmus,[31] who computed the interaction energies using the CEPA method. The CEPA method is expected to underestimate the binding indicating that our potential is the more accurate one.

[1] B. Jeziorski, R. Moszynski, and K. Szalewicz, Chem. Rev. **94**, 1887 (1994).
[2] K. Raghavachari, G. W. Trucks, J. A. Pople, and M. Head-Gordon, Chem. Phys. Lett. **157**, 479 (1989).
[3] P. J. Knowles, C. Hampel, and H.-J. Werner, J. Chem. Phys. **99**, 5219 (1993).
[4] P. J. Knowles, C. Hampel, and H.-J. Werner, J. Chem. Phys. **112**, 3106 (2000).
[5] J. D. Watts, J. Gauss, and R. J. Bartlett, J. Chem. Phys. **98**, 8718 (1993).
[6] K. Ohno, M. Yamazaki, N. Kishimoto, T. Ogawa, and K. Teakeshita, Chem. Phys. Lett. **332**, 167 (2000).
[7] M. Yamazaki, N. Kishimoto, M. Kurita, T. Ogawa, K. Ohno, and K. Teakeshita, J. Electron Spectrosc. Relat. Phenom. **114–116**, 175 (2001).
[8] M. Yamazaki, S. Maeda, N. Kishimoto, and K. Ohno, J. Chem. Phys. **117**, 5707 (2002).
[9] V. F. Lotrich and A. van der Avoird, J. Chem. Phys. **118**, 1110 (2003).
[10] W. von Niessen, J. Schirmer, and L. S. Cederbaum, Comput. Phys. Rep. **1**, 57 (1984).
[11] K. S. E. Eikema, W. Ubachs, W. Vassen, and H. Hogervorst, Phys. Rev. A **55**, 1866 (1997).
[12] G. Bieri, A. Schmelzer, L. Asbrink, and M. Jonsson, Chem. Phys. **49**, 213 (1980).
[13] M. H. Alexander, Chem. Phys. **92**, 337 (1985).
[14] M.-L. Dubernet, D. Flower, and J. M. Hutson, J. Chem. Phys. **94**, 7602 (1991).
[15] W. B. Zeimen, G. C. Groenenboom, and A. van der Avoird, J. Chem. Phys. **119**, 131 (2003).
[16] MOLPRO is a package of *ab initio* programs written by H.-J. Werner and P. J. Knowles, with contributions from J. Almlöf, R. D. Amos, A. Berning, *et al.*
[17] R. Bukowski *et al.*, *SAPT96: An Ab Initio Program for Many-Body Symmetry-Adapted Perturbation Theory Calculations of Intermolecular Interaction Energies* (University of Delaware and University of Warsaw, 1996).
[18] M. J. Frisch, G. W. Trucks, H. B. Schlegel *et al.*, GAUSSIAN 98, Revision A.7, Gaussian, Inc., Pittsburg, PA, 1998.
[19] F. B. van Duijneveldt, J. G. C. M. van Duijneveldt-van der Rijdt, and J. H. van Lenthe, Chem. Rev. (Washington, D.C.) **94**, 1873 (1994).
[20] S. F. Boys and F. Bernardi, Mol. Phys. **19**, 553 (1970).
[21] H. L. Williams, E. M. Mass, K. Szalewicz, and B. Jeziorski, J. Chem. Phys. **103**, 7374 (1995).
[22] R. Burcl, G. Chałasiński, R. Bukowski, and M. M. Szczęśniak, J. Chem. Phys. **103**, 1498 (1995).
[23] F. M. Tao and Y. K. Pan, J. Chem. Phys. **97**, 4989 (1992).
[24] F. M. Tao and Y. K. Pan, Chem. Phys. Lett. **194**, 162 (1992).
[25] The aug-cc-pVXZ basis sets were obtained from the Extensible Computational Chemistry Environment Basis Set Database, Version 1.0, as developed and distributed by the Molecular Science Computing Facility, Environmental and Molecular Sciences Laboratory which is part of the

Pacific Northwest Laboratory, P.O. Box 999, Richland, Washington 99352.
[26] R. Moszynski, P. E. S. Wormer, B. Jeziorski, and A. van der Avoird, J. Chem. Phys. **101**, 2811 (1994).
[27] C. M. Lovejoy and D. J. Nesbitt, J. Chem. Phys. **93**, 5387 (1990).
[28] W. R. Rodwell, L. T. Sin Fai Lam, and R. O. Watts, Mol. Phys. **44**, 225 (1981).
[29] A. J. Thakkar, J. Chem. Phys. **75**, 4496 (1981).
[30] S. Gewurtz, H. Lew, and P. Flainek, Can. J. Phys. **53**, 1097 (1975).
[31] T. Schmelz and P. Rosmus, Chin. Phys. Lett. **220**, 117 (1994).